Asymmetric and symmetric light couplers of daylighting systems for direct indoor lighting

2012 J. Opt. 14 125703

(http://iopscience.iop.org/2040-8986/14/12/125703)

IOP PUBLISHING JOURNAL OF OPTICS
J. Opt. **14** (2012) 125703 (7pp) doi:10.1088/2040-8978/14/12/125703

Asymmetric and symmetric light couplers of daylighting systems for direct indoor lighting

Wei-Feng Hsu, Yi-Ta Shen and I-Lin Chu

Department of Electro-optical Engineering, National Taipei University of Technology, Taipei 10608, Taiwan

E-mail: whsu@ntut.edu.tw

Received 25 April 2012, accepted for publication 17 September 2012
Published 9 October 2012
Online at stacks.iop.org/JOpt/14/125703

Abstract
Daylighting systems, which collect and transport sunlight directly into building interiors for illumination, can reduce conversion losses between different forms of energy, and thus increase the efficiency of using solar energy. To collect enough sunlight for indoor illumination, a large number of sunlight concentrators and high-efficiency light couplers are needed. In the study, we developed theoretical models of the symmetric and asymmetric Y-couplers, and conducted numerical simulations of the light couplers of three coupling angles, 10°, 30° and 50° using LightTools and Matlab. The coupling efficiencies of the asymmetric Y-couplers were 5% in average higher than those of the symmetric Y-couplers. The light couplers with a large coupling angle (50°) achieved higher coupling efficiency for the light rays of large propagation angles, and the light couplers with small coupling angles achieved 100% coupling efficiency for the light rays of small propagation angles (<24°). Therefore, the $f/\#$ of the sunlight concentrators can be calculated from the coupler parameters to reduce the angles of the light rays and thus to increase the coupling efficiency. For the branch guide to have high efficiency, the largest coupling angle of the Y-couplers was equal to the critical propagation angle 46.77°.

Keywords: solar energy, daylighting systems, light guiding, indoor lighting, light Y-couplers, coupling efficiency, asymmetric structures

(Some figures may appear in colour only in the online journal)

1. Introduction: daylighting systems for application of solar energy

Recently, great quantities of greenhouse gases have been emitted into the earth's atmosphere, resulting in global warming and dramatic climate change. A target was set for the reduction of greenhouse gas emissions that countries must strive to achieve in the third Conference of the Parties of the United Nations Climate Change Framework Convention, held in 1997 [1]. One approach toward meeting this target is to reduce the consumption of fossil fuels by using renewable energy, such as solar energy [2]. Technologies that use solar energy include photovoltaic [3–5], solar thermal [6, 7], and direct daylighting [8–15]. The first two are categorized as the active technology and have been widely developed. Direct daylighting, a passive technology, has first been classified into lighting issues in construction of buildings, but few studies in optical engineering have focused on it in spite of its advantages such as low cost, reduction of energy consumption, and healthy illumination.

A daylighting system mainly contains sunlight collectors, a light guiding system, and light emitters [8–20]. Light emitters illuminate the interiors of large structures [18–20], such as large factories, shopping malls, tunnels, and underground parking lots by using planar diffusers or light rods. Effective sunlight collectors gather solar radiation by using optical convergent components, such as a Fresnel

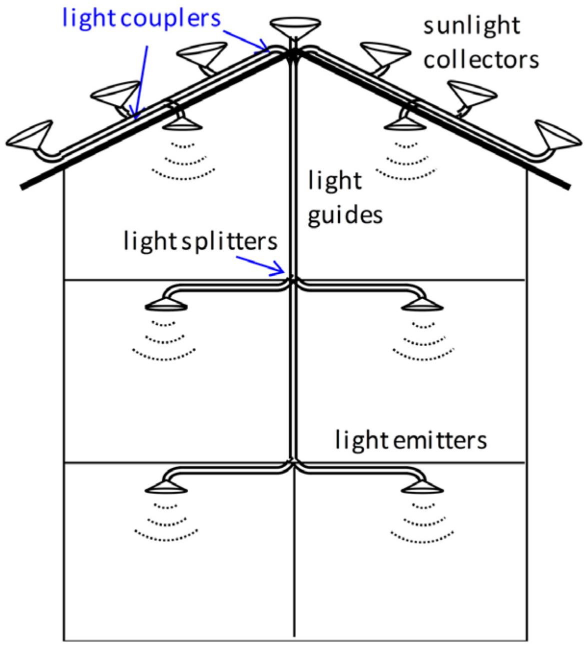

Figure 1. Schematic of a daylighting system with a building layout. Sunlight is gathered by the collectors and transferred to light emitters in a building through a light guiding system.

lens and concave reflective mirror. In cooperation with a sun-tracking device, the daylighting system can not only increase the amount of collected sunlight at different periods of the day [21–24], but also achieve a higher coupling efficiency by adjusting the orientation of the concentrators to the sun. The function of the light guiding system is to accumulate sunlight from the collectors and transfer it to the light emitters [8, 17, 21]. To accomplish this, a light guiding system consists of trunk guides, branch guides, light couplers, and decouplers. A schematic of a daylighting system with a building layout is shown in figure 1, which contains seven collectors, a system of light guides, and six light emitters for indoor lighting. The collectors are connected to the trunk guide through light couplers and the light emitters are connected through light splitters. For indoor lighting, many collectors are needed because only a limited amount of sunlight can be collected in the finite area of each collector. In addition, if uniform illumination conditions are to be produced, many light emitters are needed. The result is a need for light couplers and decouplers with high efficiency in a daylighting system.

Unlike the optical couplers in fiber communications that provide high coupling efficiency [25], the efficiency of the light couplers in daylighting systems is usually low because of the large core of the light guides. Low coupling efficiencies only slightly exceeding 50% are typical [8, 26]; that is, almost half the amount of guided sunlight is lost in coupling. This study presents a method to analyze and increase the coupling efficiency. Based on the results, asymmetrical light couplers can provide a higher coupling efficiency than symmetrical couplers. The efficiency of the light couplers significantly increases when the propagation cone of light rays is decreased using the sunlight concentrators with a large *f*-number.

2. Methodology of light couplers

Light couplers with symmetrical and asymmetrical structures were studied. A coupling circle is defined to determine whether a light ray travels through a coupling region with a coupling angle θ_{coup} [27]. The center of the coupling circle is the intersection of the extensions of the two surfaces of the coupling region, denoted as point Q in figures 2 and 3. The radius is the distance from the center Q to the farthest point at the exit of the coupling region, denoted as point P. Mirror coupling regions (MCRs) are specified every θ_{coup} above and below the coupling region. When the extension of a light ray intersects the coupling circle, the light ray travels through the coupling region, such as the blue ray in figure 2. The light path 1–2–3 is equivalent to the virtual path 1–2′–3′. The red ray, without any intersection with the coupling circle, reflects back to the entrance of the coupling region. Based on the location of the intersection R in the *m*-th MCR, we can obtain the propagation angle and the coordinate of the light ray at the exit as below.

2.1. Symmetric Y-couplers

A two-to-one light coupler with a symmetric structure, also called a symmetric Y-coupler, introduces the light rays from two entrances on one side and emits the rays at the exit on the other side, as shown in figure 2. The angle between the upper and the lower surfaces is the coupling angle θ_{coup}. At each reflection by the two surfaces, the propagation angle increases by the coupling angle θ_{coup}. When the propagation angle becomes larger than the critical propagation angle θ_{cp}, defined as

$$\theta_{cp} = (90^\circ - \theta_c), \tag{1}$$

where θ_c is the critical angle of the light guide, no more total internal reflection (TIR) occurs. The ray partially transmits to the outer region and finally disappears entirely.

Suppose that an incident ray is characterized by the propagation angle θ_{in} and the coordinate y_{in}, defined as the distance from the lower surface at the entrance of the coupler. The conjugate angle of the incident ray, θ_{cin}, is obtained by

$$\theta_{cin} = \sin^{-1}\left[2\frac{y_{in}}{W}\cos(\theta_{in})\sin\left(\frac{\theta_{coup}}{2}\right) + 2\left(1+\frac{W_{gap}}{W}\right) \times \sin\left(\theta_{in} - \frac{\theta_{coup}}{2}\right)\right] - \left(\theta_{in} - \frac{\theta_{coup}}{2}\right), \tag{2}$$

where W and W_{gap} are the width and spacing of the light guides, respectively. Using the conjugate angle, we have the coordinates (x_{cin}, y_{cin}) of the intersection R of the incident ray and the coupling circle, given by

$$(x_{cin}, y_{cin}) = \left(\frac{W + W_{gap}/2}{\tan(\theta_{coup}/2)} - \frac{W\cos\theta_{SCL}}{2\sin(\theta_{coup}/2)}, \frac{W\sin\theta_{SCL}}{2\sin(\theta_{coup}/2)}\right). \tag{3}$$

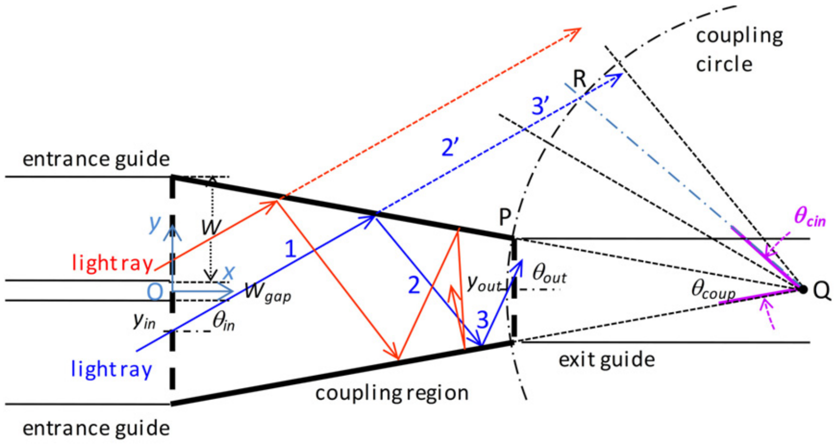

Figure 2. Symmetric Y-coupler. The blue ray travels through the coupling region and its extension intersects the coupling circle at R, located in the second mirror coupling region. The coordinate y_{out} and propagation angle θ_{out} can be found using the coupling geometrics.

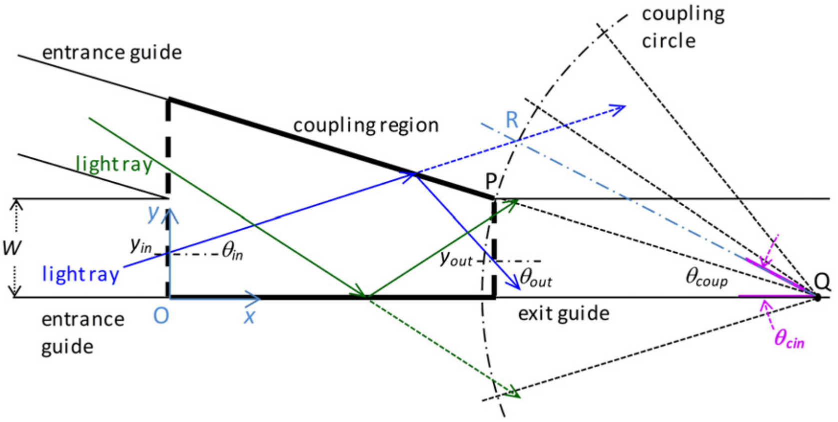

Figure 3. Asymmetric Y-coupler. The rays intersecting the coupling circle travel through the coupling region. Note that the propagation angle increases only when the ray reflects by the tilted surface such as the blue ray, while the propagation angle of the green ray does not change.

The total number of reflections of the light ray traveling in the symmetric coupling region is calculated by

$$m = \lfloor \theta_{\mathrm{cin}}/\theta_{\mathrm{coup}} \rfloor, \tag{4}$$

where $\lfloor p \rfloor$ denotes the largest integer less than or equal to p. The propagation angle at the exit, θ_{out}, is then obtained as

$$\theta_{\mathrm{out}} = (1 - 4(m/2 - \lfloor m/2 \rfloor)) \times (\theta_{\mathrm{in}} + 2m\theta_{\mathrm{coup}}). \tag{5}$$

The coordinate of the ray at the exit, y_{out}, is obtained as

$$y_{\mathrm{out}} = \frac{W}{2}\left(1 - \frac{\theta_{\mathrm{in}}}{|\theta_{\mathrm{in}}|}\right) + \left(\left|\frac{x_{\mathrm{cin}}}{\tan(2m\theta_{\mathrm{coup}})} - y_{\mathrm{cin}} - \left(X_{\mathrm{coup}} + \frac{W\tan(\theta_{\mathrm{coup}})}{2}\right) \Big/ \tan(2m\theta_{\mathrm{coup}})\right|\right) \times \left(\sqrt{(1/\tan(2m\theta_{\mathrm{coup}}))^2 + 1}\right)^{-1} \times \frac{\theta_{\mathrm{in}}}{|\theta_{\mathrm{in}}|}, \tag{6}$$

where X_{coup} is the length of the coupling region, given by

$$X_{\mathrm{coup}} = \tfrac{1}{2}\left(W + W_{\mathrm{gap}}\right)\cot\left(\theta_{\mathrm{coup}}/2\right). \tag{7}$$

2.2. Asymmetric Y-couplers

In an asymmetric two-to-one light coupler, the exit guide is an extension of one entrance guide, called the trunk guide, and the other light guide, called the branch guide, enters at a tilted angle that is defined as the coupling angle θ_{coup}. We term it an asymmetric Y-coupler, which is shown in figure 3. When a light ray travels through the coupling region, the propagation angle only increases at one of the surfaces. Therefore, light rays can travel longer distances. In addition, the coupling efficiencies of the two entrance guides are different, which provides flexibility in the design of light couplers.

Similarly, suppose that the propagation angle and the coordinate of an incident ray are θ_{in} and y_{in}, respectively. Using the geometry of figure 3, we find the conjugate angle of the incident ray, θ_{cin}, given by

$$\theta_{\mathrm{cin}} = \sin^{-1}\left[\frac{y_{\mathrm{in}}}{W}\cos(\theta_{\mathrm{in}})\sin(\theta_{\mathrm{coup}}) + \sin(\theta_{\mathrm{in}}) \times (1 + \cos(\theta_{\mathrm{coup}}))\right] - \theta_{\mathrm{in}}, \tag{8}$$

where W is the width of the light guides. The coordinates $(x_{\mathrm{cin}}, y_{\mathrm{cin}})$ of the intersection R of the incident ray and the coupling circle are obtained by

$$(x_{\mathrm{cin}}, y_{\mathrm{cin}}) = \left(\frac{2W}{\tan(\theta_{\mathrm{coup}})} - \frac{W\cos\theta_{\mathrm{cin}}}{\sin(\theta_{\mathrm{coup}})}, \frac{W\sin\theta_{\mathrm{cin}}}{\sin(\theta_{\mathrm{coup}})} \right). \quad (9)$$

The total number of reflections of a light ray traveling in the asymmetric coupling region is obtained by

$$m = 2 \times |\lfloor \theta_{\mathrm{cin}}/\theta_{\mathrm{coup}} \rfloor /2|. \quad (10)$$

Note that only the reflections at the upper surface affect the propagation angle, and the propagation angle at the exit of the coupler is expressed as

$$\theta_{\mathrm{out}} = (1 - 4(m/2 - \lfloor m/2 \rfloor))(\theta_{\mathrm{in}} + 2\lfloor m/2 \rfloor \theta_{\mathrm{coup}}). \quad (11)$$

The output coordinate y_{out} of the ray is finally obtained as

$$\begin{aligned} y_{\mathrm{out}} = {} & (|x_{\mathrm{cin}}/\tan(m\theta_{\mathrm{coup}}) - y_{\mathrm{cin}} \\ & - W(1+\cos(\theta_{\mathrm{coup}}))/\sin(\theta_{\mathrm{coup}})/\tan(m\theta_{\mathrm{coup}})|) \\ & \times \left(\sqrt{(1/\tan(m\theta_{\mathrm{coup}})^2) + 1} \right)^{-1}. \end{aligned} \quad (12)$$

2.3. Coupling efficiency

The coupling loss of light is derived mainly from the effect of TIR. When a light ray travels through a coupler, the propagation angle of the light ray increases because of the reflection of the tilted surfaces of the coupler. When the propagation angle is larger than the critical propagation angle, as defined in (1), the ray leaves the light guide. We ignore the losses coming from the scattering and absorption of the guide material because the coupler is small in length.

Two coupling efficiencies are defined here. The angular coupling efficiency of the light rays with a certain propagation angle θ at the entrance of the coupler is defined as

$$\Delta\eta_\theta = \frac{L_{\mathrm{out}}(\theta)}{L_{\mathrm{in}}(\theta)}, \quad (13)$$

where $L_{\mathrm{out}}(\theta)$ and $L_{\mathrm{in}}(\theta)$ are the illuminance (lux) of the incident rays with propagation angle θ at the entrance and the exit of the coupler, respectively. The accumulated coupling efficiency $\eta_{\theta\mathrm{in}}$ is defined as

$$\eta_{\theta_{\mathrm{in}}} \equiv \frac{\int_{-\theta_{\mathrm{in}}}^{\theta_{\mathrm{in}}} L_{\mathrm{out}}(\theta)\,\mathrm{d}\theta}{\int_{-\theta_{\mathrm{in}}}^{\theta_{\mathrm{in}}} L_{\mathrm{in}}(\theta)\,\mathrm{d}\theta} = \frac{1}{2\theta_{\mathrm{in}}} \int_{-\theta_{\mathrm{in}}}^{\theta_{\mathrm{in}}} \Delta\eta_\theta\,\mathrm{d}\theta. \quad (14)$$

2.4. Daylight factor (DF)

The daylight factor (DF) is used to evaluate the luminous efficacy of a daylighting system [10–12]. The DF is defined as the ratio of inside illuminance L_{inside} (lux) at the light emitter surface and outside illuminance L_{outside} (lux) on the sunlight concentrator plane, which is given by

$$\mathrm{DF} = \frac{L_{\mathrm{inside}}}{L_{\mathrm{outside}}}. \quad (15)$$

To illustrate the relationship between DF and $\eta_{\theta\mathrm{in}}$, we consider a daylighting system containing N sunlight concentrators with a concentrating factor η_{c} and one light emitter with a diffuse factor η_{e}. The concentrators and emitter are connected by a light guiding system with $(N-1)$ light couplers. The efficiencies of the trunk guide and the branch guide of the light coupler are η_{t} and η_{b}, respectively. For simplicity, the transmission losses of the light guides between contractors, couplers and emitter are neglected, and therefore the inside illuminance can be calculated by the product of the outside illuminance and the accumulation of these factors, giving

$$L_{\mathrm{inside}} = L_{\mathrm{outside}}\eta_{\mathrm{c}}\eta_{\mathrm{e}}\eta_{\mathrm{b}} \sum_{n=0}^{N-1} \eta_{\mathrm{t}}^n. \quad (16)$$

The DF of the daylighting system with $(N-1)$ asymmetric Y-couplers is then expressed by

$$DF_{\mathrm{asy}} = \eta_{\mathrm{c}}\eta_{\mathrm{e}}\eta_{\mathrm{b}} \sum_{n=0}^{N-1} \eta_{\mathrm{t}}^n. \quad (17)$$

For the symmetric Y-couplers, $\eta_{\mathrm{t}} = \eta_{\mathrm{b}}$ $(=\eta_{\theta\mathrm{in}})$, and the DF of the daylighting system is expressed by

$$DF_{\mathrm{sym}} = \eta_{\mathrm{c}}\eta_{\mathrm{e}} \sum_{n=1}^{N} \eta_{\mathrm{t}}^n. \quad (18)$$

In (17) and (18) the efficiencies of the light couplers, η_{t} and η_{b}, dominate the DF of a light guiding system with multiple light couplers, especially the efficiency from the trunk guide η_{t}.

3. Simulations and discussions

The simulations of light couplers were conducted using Matlab and Lighttools, and both results were consistent. The analysis of the simulation data is mainly obtained by using LightTools, and the Matlab results were analyzed in details to improve the coupling efficiencies. In the simulations, we assumed the dimension of the light guide was 4 mm, and the interior and surrounding of the couplers were 1.460 and 1.000 (air), respectively. This resulted in a critical angle (θ_{c}) of 43.23° and a critical propagation angle (θ_{cp}) of 46.77° in the light guide. Three coupling angles, 10°, 30° and 50°, of the light couplers were compared to show the significance of the use of asymmetric Y-couplers in sunlight guiding systems.

3.1. Angular coupling efficiency ($\Delta\eta_\theta$)

The angular coupling efficiency is the ratio of the output flux to the input flux of a specific angle (θ) of the incident rays. Because the losses of light rays result from the increase of the propagation angle after reflections, the efficiency profile is reciprocally symmetrical to $\theta_{\mathrm{in,air}} = 0°$ for the two entrance guides of the symmetric coupler, as shown in figures 4(a)–(c). For asymmetric light couplers, however, the angular coupling efficiencies of the trunk guide are larger than those of the branch guide, as shown in figures 4(d)–(f). Figure 4 shows that a great amount of light rays with small propagation

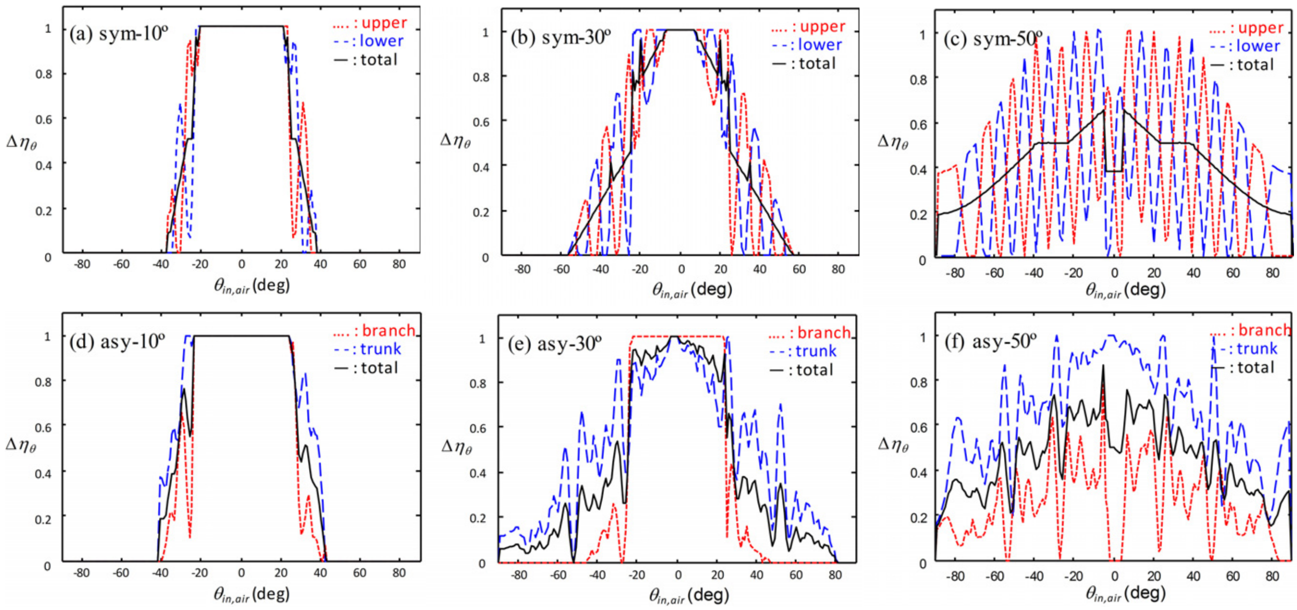

Figure 4. Angular coupling efficiency of symmetric and asymmetric Y-couplers with coupling angles of 10°, 30° and 50°. The efficiency profiles of the two entrance guides of the symmetric Y-coupler are similar, as shown in (a)–(c). For the asymmetric Y-couplers, the efficiency profiles of the trunk and the branch guides are considerably different, as shown in (d)–(f).

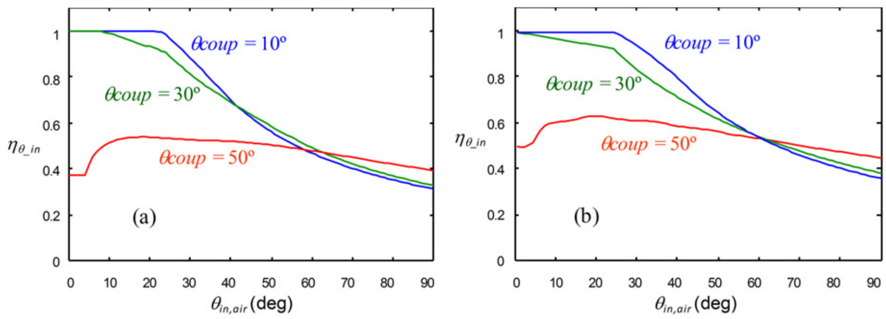

Figure 5. Accumulated coupling efficiency of symmetric and asymmetric Y-couplers with coupling angles of 10°, 30° and 50°.

angles can travel through the coupling regions with small coupling angles such as 10° and 30°. For the couplers of large coupling angle (50°), the rays of small propagation angles are mostly rejected, especially for the rays from the branch guide, because the new propagation angles exceed the critical propagation angle.

According to the results shown in figure 4, one might choose sunlight concentrators of large *f*-numbers to collect sunlight and light couplers of small coupling angles for a daylighting system because of the large angular coupling efficiency of the light rays of small propagation angles. Note that, however, the propagation angle of light rays increases when the rays travel through the coupling region. The propagation angles of the light rays traveling in the trunk guide are in range of all possible angles in the critical propagation angle, or corresponding to 90° of the incident angle in air. Therefore, the accumulated coupling efficiencies of the light couplers are of particular interest in the designs of light couplers.

3.2. Accumulated coupling efficiency ($\eta_{\theta\_\mathrm{in}}$)

The total amount of sunlight transmitted to the exit of a coupler takes into account the light rays in all propagation angles, which is illustrated by the accumulated coupling efficiency, as defined in (14). The accumulated coupling efficiency is calculated by averaging the angular coupling efficiencies in the propagation cone. The accumulated coupling efficiencies of the six light couplers are shown in figure 5. As shown in table 1, the accumulated coupling efficiencies of the asymmetric couplers are higher than those of symmetric couplers of the same coupling angles. With the angle of the incident rays uniformly distributed in ±90° ($\theta_{\mathrm{in\_air}}$), the accumulated coupling efficiencies are in general low, as shown in table 1, and the largest $\eta_{90°}$ is 0.448 for the 50°–θ_{coup} asymmetric coupler. In spite of the asymmetric Y-couplers having higher coupling efficiencies than the symmetric Y-couplers, the coupling efficiencies of both couplers are inadequate for daylighting applications because more than 50% of the transported light is lost.

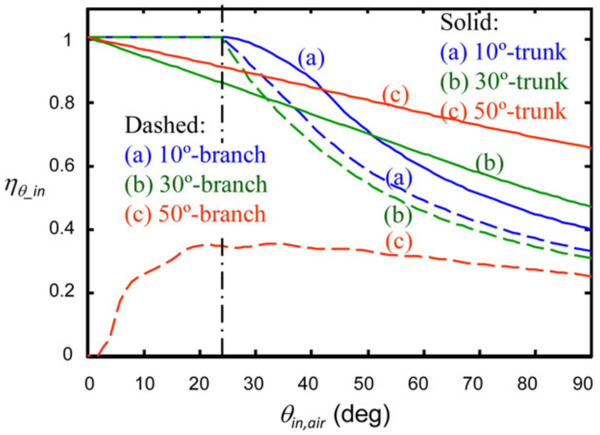

Figure 6. Accumulated coupling efficiency of individual light guides of asymmetric Y-couplers with coupling angles of 10°, 30° and 50°. The dash–dotted line indicates the incident angle (in air) to the light guide which can provide the highest coupling efficiency. It is 24° here and is used to specify the $f/\#$ of the sunlight concentrator.

Table 1. Accumulated coupling efficiency ($\eta_{\theta\_\mathrm{in}}$).

	Symmetric Y		Asymmetric Y	
θ_{coup} (deg)	$\eta_{20°}$	$\eta_{90°}$	$\eta_{20°}$	$\eta_{90°}$
10	1.000	0.316	1.000	0.361
30	0.935	0.333	0.940	0.385
50	0.537	0.394	0.633	0.448

Most daylighting systems use concentrating collectors, specified by an f-number ($f/\#$), to increase the collected sunlight, which results in an incident cone with the largest angle $\theta_{\mathrm{in,air}}$. When $f/1.37$ concentrators are used (i.e., $\theta_{\mathrm{in,air}} = 20°$), the largest $\eta_{\theta\mathrm{in\_air}}$ is 1.000 for both symmetric and asymmetric couplers with 10° coupling angle, as shown in table 1. As the f-number of the sunlight concentrator increases, the incident cone to the light guide becomes narrower and the accumulated coupling efficiency increases.

3.3. High-efficiency light couplers and sunlight concentrators

In table 1, the $\eta_{20°}$ values of the two 50°–θ_{coup} couplers are much lower than those of 10°–θ_{coup} and 30°–θ_{coup} couplers. To illustrate this phenomenon, the accumulated coupling efficiencies of each entrance guide of the asymmetric Y-couplers are shown as in figure 6. Note that for the symmetric Y-couplers the $\eta_{\theta\_\mathrm{in}}$ of each entrance guides is identical and the $\eta_{\theta\_\mathrm{in}}$ of the coupler is as well. Figure 5(a) is then used to show the $\eta_{\theta\_\mathrm{in}}$ of individual entrance guides of the symmetric Y-couplers.

Table 2 lists some typical values in figures 5(a) and 6. When the coupling angle increases, the $\eta_{90°}$ of the trunk guides increases because of the decrease of the coupling regions in length, and the $\eta_{90°}$ of the branch guides decreases because of the great increase of the propagation angle. The rapid drop of the efficiency of the branch guide of different couplers results from the reflective angle of the

Table 2. Accumulated coupling efficiency ($\eta_{\theta\_\mathrm{in}}$) of the light guides of the asymmetric Y-couplers.

	Trunk guide		Branch guide		Total	
θ_{coup} (deg)	$\eta_{24°}$	$\eta_{90°}$	$\eta_{24°}$	$\eta_{90°}$	$\eta_{24°}$	$\eta_{90°}$
10	1.000	0.395	1.000	0.326	1.000	0.361
30	0.856	0.466	0.998	0.303	0.927	0.385
50	0.906	0.648	0.342	0.247	0.624	0.448

normal propagation ray exceeding the critical propagation angle. To provide high coupling efficiency of the branch guide, the coupling angle is suggested to be less than the critical propagation angle; that is, 46.77° here. To provide high coupling efficiency of the light couplers, sunlight concentrators with an f-number greater than 1.1 are suggested in a daylighting system. The value of f-number is given by

$$f/\# = \frac{1}{2\tan\{\sin^{-1}[n_{\mathrm{guide}}\sin(\theta_{\mathrm{cp}} - m\theta_{\mathrm{coup}})]\}}, \qquad (19)$$

where n_{guide} is the refractive index of the light guide, and the corresponding angle in air is 24° here, as denoted by a dash–dotted line in figure 6.

4. Conclusion

As great quantities of greenhouse gases have been emitted into the earth's atmosphere, resulting in global warming and dramatic climate change, the effective use of solar energy has become a critical issue. In recent years, many technologies of solar energy usage have been developed, such as photovoltaic, solar thermal, and direct daylighting. Daylighting systems, which collect and transport sunlight directly into building interiors for indoor illumination, can reduce the conversion losses between different forms of energy and, thus, increase the efficiency of using solar energy.

A daylighting system consists of sunlight collectors, a light guiding system, and light emitters. To collect enough sunlight for indoor illumination, a large number of sunlight collectors and high-efficiency light couplers are needed. To increase the coupling efficiency of the light couplers, we developed theoretical models of the symmetric and asymmetric light couplers, and conducted numerical simulations of light Y-couplers of 10°, 30° and 50° coupling angles using Matlab and Lighttools. Based on the simulation results, asymmetric Y-couplers provide higher coupling efficiencies than do symmetric Y-couplers (5% on average). The profiles of the accumulated coupling efficiency of the branch guides show that the coupling angle should not exceed the critical propagation angle (46.77°) for the light from the branch guide transferred to the exit guide.

When the traveling rays of all possible propagation angles (in θ_{cp}) enter into the coupling region, couplers with a large coupling angle provide a higher coupling efficiency than couplers with small angles do. However, the coupling efficiencies of both couplers are typically low (<0.5). These results suggest that the propagation angles of the traveling rays be compressed to achieve a high coupling efficiency.

The optimum coupling efficiency ($\eta_{\theta\text{in}} = 1.0$) is achieved when the largest incident angle (in air) of the traveling rays is 24° in the light couplers with $\theta_{\text{coup}} = 10°$. Using the $f/\#$ of the sunlight concentrators, determined by the refractive index, the critical propagation angle and the coupling angle, the Y-couplers can achieve such high coupling efficiencies.

References

[1] United Nations 1997 *Kyoto Protocol to the United Nations: Framework Convention on the Climate Change (Kyoto)*
[2] Byrne J, Kurdgelashvili L, Mathai M V, Kumar A, Yu J-M, Zhang X, Tian J, Rickerson W and Timilsina G R 2010 *World Solar Energy Review: Technology, Markets and Policies* (Newark, DE: University of Delaware)
[3] Shah A, Torres P, Tscharner R, Wyrsch N and Keppner H 1999 *Science* **285** 692–8
[4] Sun G, Chang F and Sorel R A 2010 *Opt. Express* **18** 3746–53
[5] Li G, Zhu R and Yang Y 2012 *Nature Photon.* **6** 153–61
[6] Murthy M V R 2009 *Renew. Sustain. Energy Rev.* **13** 835–44
[7] Thirugnanasambandam M, Iniyan S and Goic R 2010 *Renew. Sustain. Energy Rev.* **14** 312–22
[8] Fraas L M, Pyle W R and Ryason P R 1983 *Appl. Opt.* **22** 578–82
[9] Kischkoweit-Lopin M 2002 *Sol. Energy* **73** 77–82
[10] Scartezzini J-L and Courret G 2004 *Proc. SPIE* **5185** 35–48
[11] Chel A, Tiwari G N and Chandra A 2009 *Appl. Energy* **86** 2507–19
[12] Chel A, Tiwari G N and Singh H N 2010 *Appl. Energy* **87** 3037–50
[13] Kim J T and Kim G 2010 *Build. Environ.* **45** 256–69
[14] Shi L and Chew M Y L 2012 *Renew. Sustain. Energy Rev.* **16** 192–207
[15] Mayhoub M and Carter D 2012 *Build. Environ.* **53** 83–94
[16] Lo Verso V R M, Pellegrino A and Serra V 2011 *Sol. Energy* **85** 2789–801
[17] Tsangrassoulis A *et al* 2005 *Sol. Energy* **79** 56–64
[18] Rosemann A and Kaase H 2005 *Sol. Energy* **78** 772–80
[19] Nakamura T 2009 *Proc. SPIE* **7423** 74230C
[20] Whang A J-W, Chen Y-Y, Yang S-H, Pan P H, Chou K-H, Lee Y-C, Lee Z-Y, Chen C-A and Chen C-N 2010 *Appl. Opt.* **49** 6789–801
[21] Francini F, Fontani D, Jafrancesco D, Mercatelli L and Sansoni P 2006 *Proc. SPIE* **6338** 63380O
[22] Mousazadeh H, Keyhani A, Javadi A, Mobli H, Abrinia K and Sharifi A 2009 *Renew. Sustain. Energy Rev.* **13** 1800–18
[23] Rumyantsev V D 2010 *Opt. Express* **18** A17–24
[24] Zhang D, Castor J M and Kostuk R K 2011 *J. Photon. Energy* **1** 015505
[25] Ehsan A A, Shaari S and Rahman M K A 2010 *Prog. Electromagn. Res.* **101** 1–16
[26] Zik O, Karni J and Kribus A 1999 *Sol. Energy* **67** 13–22
[27] Winston R, Minano J C, Benitez P, Shatz N and Bortz J C 2005 *Nonimaging Optics* (Oxford: Elsevier Academic)